GRAPHENE-ABS NANOCOMPOSITES FOR FUSED DEPOSITION MODELLING

Sithiprumnea Dul, Haroon Mahmood, Luca Fambri, Alessandro Pegoretti

Department of Industrial Engineering and INSTM Research Unit, University of Trento, Via Sommarive 9, 38123 Trento, Italy
Email: sithiprumnea.dul@unitn.it, haroon.mahmood@unitn.it, luca.fambri@unitn.it, alessandro.pegoretti@unitn.it,
Web Page: http://www.unitn.it

Keywords: ABS; Fused deposition modelling; Nanocomposite; Graphene nanoplatelets; mechanical properties

Abstract

Graphene nanoplatelets (xGnP) were incorporated at a content of 4 and 8 wt% into two types of acrylonitrile-butadiene-styrene (ABS) with and without mould lubricant in order to select the most convenient composition for fused deposition modelling (FDM). After comparison of tensile and flow properties of compression moulded, the compositions of ABS with lubricant up to 4 wt% of graphene were melt compounded and used for extrusion of filaments for feeding a commercial FDM machine. Thermo-mechanical properties of FDM samples at different build orientation were investigated, through quasi-static tensile test, dynamic mechanical thermal analysis (DMTA) and creep test of neat ABS and its nanocomposite. Elastic modulus and dynamic storage moduli of printed parts were significantly improved by the presence of graphene. As a side effect, ultimate strength and elongation at break decreased due to lack of adhesion between xGnP and ABS which was proved by FESEM observations. Moreover, xGnP promoted a better thermal stability of 3D-components as evidenced by the reduction of both coefficient of linear thermal expansion and creep compliance. Graphene exhibits better reinforcing effect for the horizontal build orientation in comparison to perpendicular printed specimens.

1. Introduction

Fused deposition modelling (FDM) is the most widely diffused additive manufacture technology. Development of composite materials for fused deposition modelling (FDM) offers a challenge for enhancing the properties of 3D-printed components [1]. Recently, nanocomposite has been an active research area as innovative materials due to improved material properties by adding small amount of nanofiller. Graphene nanoplatelets (xGnP) are considered as potential reinforcing filler since it possesses 2D graphene stacked structures. Therefore graphene nanocomposite shows enhanced mechanical and thermal properties in thermoplastic materials [2-4]. By far, only one study of FDM of graphene as filler in ABS feedstock through solution mixing has been reported in past [5]. However, not only were the mechanical properties investigated, but also a very small decrease (~4%) of coefficient of dilation were reported.

One of most frequently used thermoplastic for FDM is acrylonitrile-butadiene-styrene (ABS) due to its desirable properties such as easy processing characteristics, chemical resistance, toughness, dimensional stability and good surface appearance. However, it has some drawbacks including poor flame resistance, thermal stability, and low mechanical properties in comparison of other engineering plastics [6]. The flow and processability of ABS determined by characteristics of base resin and also the effect of additive of various kinds (e.g. lubricant, impact modifier, stabilizers, and filler). Filler additive generally limited the processability due to increasing the viscosity of polymeric matrix. On the other hand, molding lubricant additive significant affects viscosity of ABS, therefore it promotes the processability by preventing sticking to processing equipment [7].

Excerpt from ISBN 978-3-00-053387-7

In the present work, graphene-ABS filament nanocomposite were used through a procedure of solvent-free melt compounding following by extrusion. ABS copolymer with and without lubricant additive nanocomposite were preliminary studied in order to selected the suitable filament for FDM. The effect of xGnP on ABS 3D-printed parts was investigated under thermo-mechanical properties along different build orientations (i.e. horizontal and perpendicular).

2. Materials and methods

2.1. Materials and processing

Two type of acrylonitrile-butadiene-styrene (ABS) copolymer with tradename Sinkral®L322 and Sinkral®F322 with and without mould lubricant respectively were used as matrix in this study provided by Versalis S.p.A. (Mantova, Italy) in form of white pellets. Graphene nanoplatelets (xGnP) were purchased from XG Sciences (East Lansing, MI). For the selected type of nanoplatelets (type M5), the manufacturer reports average lateral dimension of 5 μm, thickness of 6-8 nm, and surface area of 120-150 m²/g.
The graphene nanoplatelets (xGnP) of 4 and 8 wt% were to be incorporated into ABS matrix. Pellets of ABS were first melt compounded followed by addition of xGnP using a Thermo-82 Haake Polylab Rheomix having counter-rotating internal mixer at 190 °C and rotor speed 90 rpm for 15 min. Neat ABS was also processed under the same conditions. The resulting material were hot pressed in a Carver Laboratory press under a pressure of 3.9 MPa to obtain the square sheet. The plate samples were denoted indicating the nanofiller mass fraction and the type of matrix. As an example, G8-L322 indicates the plate nanocomposite of ABS Sinkral®L322 with 8 wt% of graphene.
For FDM specimen preparation, the blended materials were granulated by using Piovan grinder Model RN 166. Granulated materials were used to feed a Thermo Haake PTW16 intermeshing co-rotating twin screw extruder (screw diameter=16 mm; L/D ratio=25; rod die diameter 3 mm). The temperature profile along the screw was gradually increased from 180 °C to 200 °C at rod die. The monofilament of 1.75 ± 0.10 mm were collected by a take-off unit Thermo Electron Type 002-5341. 3D printed specimens were manufactured by a Sharebot Next Generation desktop 3D printer (Sharebot NG, Italy) feed with the filaments. Dog-bone and parallelepiped specimens were built-up along two orientations, i.e. horizontal (H) and perpendicular (P), as shown in **Figure 1**. Printing parameters were conducted through Slic3r software as follows: concentric infill type; object infill 100%; no raft; nozzle diameter 0.35 mm; layer height 0.20 mm; nozzle temperature 230 °C; bed temperature 60 °C. The infill rate was fixed at 40 mm/s for H, whereas P specimens were produced at lower deposition rate (4 mm/s). Printed samples were denoted indicating the nanofiller mass fraction, the type of matrix, and build orientation. For instance, G4-L322-P indicates the nanocomposite of ABS Sinkral®L322 with 4 wt% of graphene, printed at perpendicular orientation.

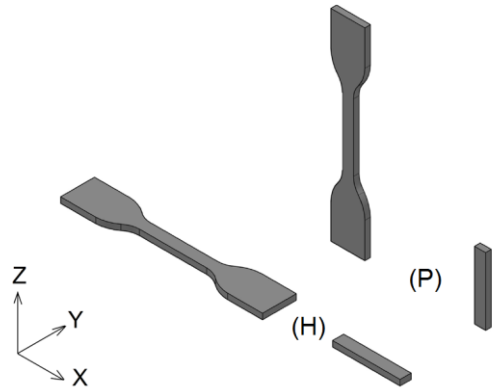

Figure 1. Schematic of 3D-printed dog-bone and parallelepiped specimens at horizontal (H) and perpendicular (P) build orientation.

Excerpt from ISBN 978-3-00-053387-7

2.4. Testing techniques

Differential scanning calorimetry (DSC) analysis was performed by a Mettler DSC 30 calorimeter under nitrogen flow of 100 ml/min on samples with a mass of about 10 mg. The samples were tested under heating-cooling-heating cycle in the range 30 °C - 260 °C at a rate of ±10 °C /min. Fourier transform infrared (FTIR) spectra were recorded by a Spectrum One™ spectrometer (Perkin Elmer ATR-FTIR). The fracture surfaces of specimens were observed by using a Carl Zeiss AG Supra 40 field emission scanning electron microscope (FESEM) at an acceleration voltage of 5 kV; specimens were broken in a brittle manner after immersed in liquid nitrogen for about 60 min. Uniaxial tensile tests were performed at room temperature by an Instron® 5969 electromechanical testing machine equipped with a 50 kN load cell. The yield and fracture points were evaluated at a crosshead speed of 10 mm/min. 3D printed materials (H and P) for dog-bone specimens based on the standard ISO 527 type 5A (gauge length 25 mm; thickness 2 mm). Elastic modulus of 3D-printed specimens was determined at a cross-head speed of 1 mm/min by an electrical extensometer Instron® model 2620-601 with a gage length of 12.5 mm. According to ISO 527 standard, the elastic modulus was determined as a secant value between strain levels of 0.05% and 0.25%. The tensile data were reported as average value of at least three replicates. Dynamic mechanical thermal analysis (DMTA) was carried out under tensile mode by a TA Instruments DMA Q800 device from -100°C to 150 °C at a heating rate of 3°C/min applying a dynamic maximum strain of 0.05% at a frequency of 1 Hz. Parallelepiped specimens were tested having a length of 25 mm and different cross section (width 4 mm and a thickness 2 mm). The gauge length of all samples was fixed at 11.8 mm. Storage modulus (E') and loss modulus (E'') were reported. Glass transition was determined as the maximum of the loss modulus peak (tan δ). Coefficient of linear thermal expansion (CTE) was determined from the thermal strain according to equation (Eq.1):

$$CTE = \frac{\Delta L / L_0}{\Delta T} \tag{1}$$

where L_0 and ΔL are the initial specimen gauge length and the length variation, and ΔT is the selected temperature interval (i.e. -40/-10°C and 10/40°C). Creep test were performed through a TA Instruments DMA Q800 under a constant stress of 3.9 MPa, corresponding 10% of yield stress of neat ABS, at 30 °C up to 3600 s. Rectangular specimens with length of 25 mm, width of 4 mm and thickness of 1 mm were also prepared by 3D printing. The adopted gauge of all samples was 11.8 mm.

3. Results and discussions

Figure 2 shows the typical DSC thermograms of different type of ABS matrix from compression moulding. We can clearly differential these two ABS by an endothermic peak presenting in L322 at temperature 138 ºC (in **Table 1**) which is associated to additive mould lubricant. The lubricant could be fatty acid amide (FAA) which has melting point of 150 ºC, in conformity to literature [7]. From **Table 2**, both ABS have glass transition temperature about 100 ºC indicating styrene–acrylonitrile copolymer phase (SAN). FTIR spectra of ABS-graphene nanocomposites and matrices from compression moulding are shown in **Figure 3**. The presence of graphene does not dominant over ABS matrix because there are no addition peak, but spectra with L322 clearly show the presence of different peaks related to mould lubricant additive at ~3296, 1638 and 1555 cm^{-1} which correspond to N-H, and C=O stretch of amide group, respectively. Based on DSC and FTIR, the mould lubricant additive suggested to be fatty acid amide.

Excerpt from ISBN 978-3-00-053387-7

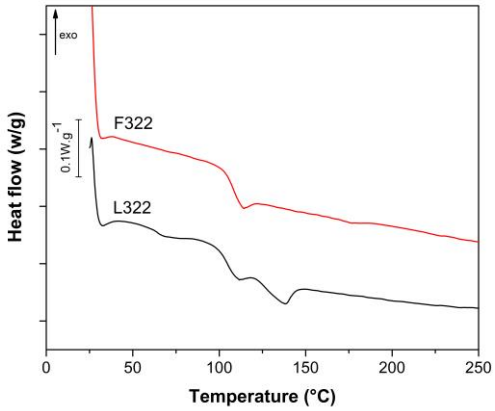

Figure 2. DSC thermograms of neat ABS and nanocomposite of compression moulded (CM) samples at first heating scan.

Table 1. Glass transition temperatures (T_g) and heat capacity (ΔC_p) of styrene–acrylonitrile phase, and interval melting temperature (ΔT_m) and melting temperature (T_m) of mould lubricant for ABS.

Sample	First heating				Second heating			
	T_g* (°C)	ΔC_p (J/gK)	ΔT_m (°C)	T_m (°C)	T_g* (°C)	ΔC_p (J/gK)	ΔT_m (°C)	T_m (°C)
L322	99	0.372	120-150	138	101	0.355	120-150	138
F322	103	0.367	-	-	103	0.378	-	-

* T_g value were evaluated by onset temperature.

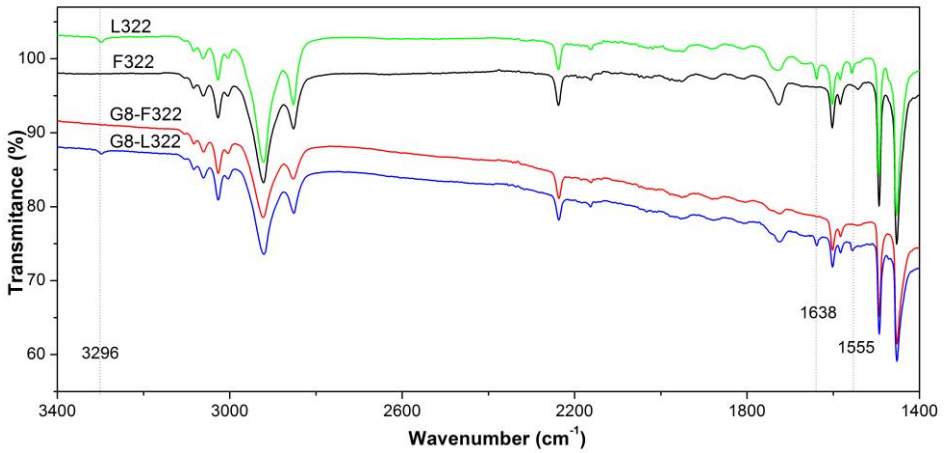

Figure 3. FTIR spectra of compression mould specimens of ABS nanocomposites.

Figure 4a-c shows the tensile properties of ABS nanocomposite. Elastic modulus and tensile strength of neat F322 is slightly higher than L322 specimens which could attributed to additive mould lubricant. By adding graphene the elastic modulus were shown the improvement for both ABS, while tensile strength of F322 shows fairly constant, but L322 exhibits a slightly reduction. Melt flow index is a key parameter for processing properties. A significant reduction in MFI value of ABS by presence of graphene due to restriction of mobility chain is depicted in **Figure 4**d. Moreover, L322 matrix and its nanocomposite show higher MFI value than correspondent materials based on F322. In particular, the MFI ratio of L322 over F322 is 1.47 for pure matrix, whereas 1.62 and 1.81 for nanocomposite at 4 and 8 wt% of graphene, respectively. Similarly, the viscosity ratio of 1.56 for pure ABS were reported [7]. Consequently, from these findings ABS L322 with and without graphene 4 wt% has been selected for FDM process.

Excerpt from ISBN 978-3-00-053387-7

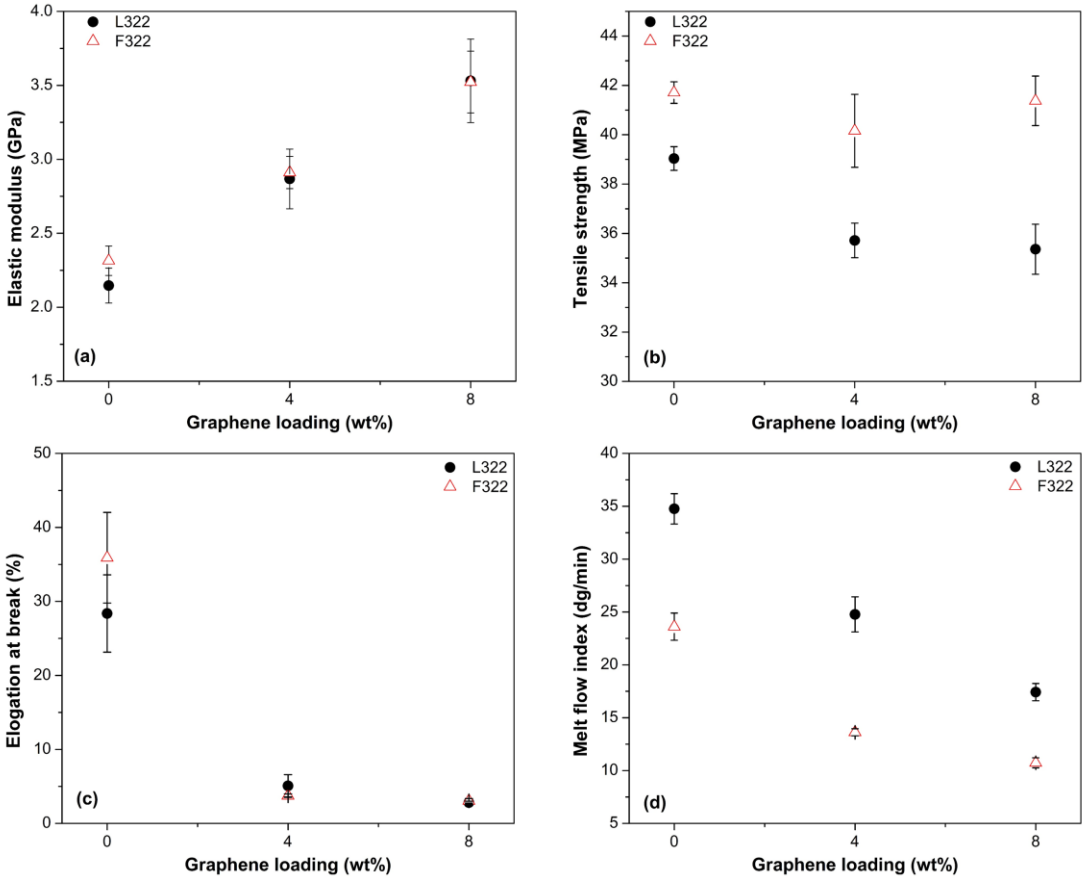

Figure 4. Tensile and flow properties of nanocomposite of compression molding specimen, (a) Elastic modulus, (b) tensile strength, (c) elongation at break and (d) melt flow index.

FESEM micrograph at high magnification of the fracture surface of dog-bone specimens of horizontal and perpendicular build nanocomposite are shown in **Figure 5**a and b respectively. A poor adhesion level between graphene and ABS matrix is observed as in **Figure 5**b. Moreover, graphene nanoplatelets in H specimen appear to be perpendicular fracture plane, therefore most likely oriented along the loading direction of specimen. On the hand, **Figure 5**a shows the graphene nanoplatelets in P specimen are likely to be distributed parallel to the cross-section. It can be therefore inferred that during FDM process, graphene flakes were oriented parallel along each single deposited filaments.

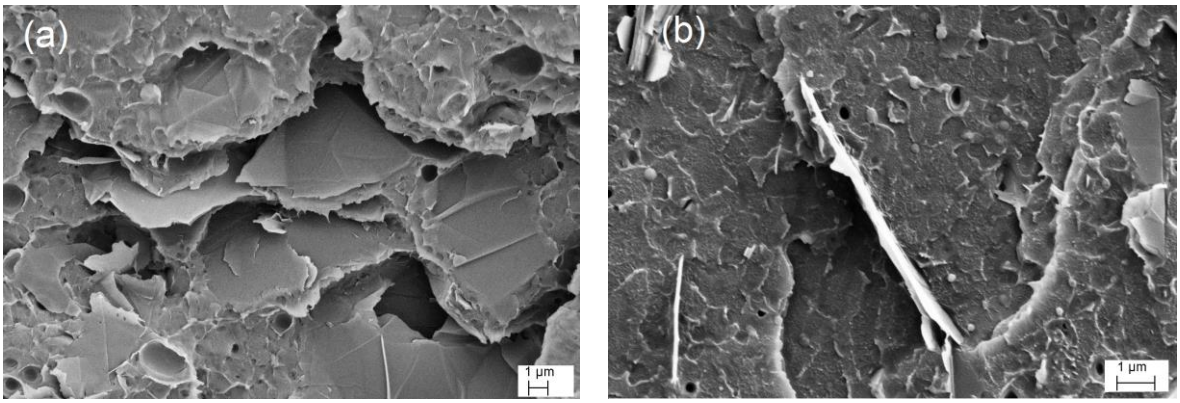

Figure 5. SEM micrograph of 3D printed dog-bone specimens, G4-L322-P (a), and G4-L322-H (b).

Graphene nanoplatelets significantly affect the tensile properties of 3D-printed parts. **Figure 6** shows the stress-strain curve of representative FDM specimens. Elastic modulus, yield and fracture point with

Excerpt from ISBN 978-3-00-053387-7

H and P build orientation are shown in **Table 2**. 3D-printed specimens exposure the yield points for neat ABS, while adding graphene samples show the brittle behavior. Horizontal samples showed higher elastic modulus, maximum stress, and stain at break than perpendicular samples. The behavior occurred for H specimens due to deposition filaments aligned along tensile load whereas that of P specimen is oriented transversally to the tensile load. According to literatures, some previous studies reported the similar trends of the comparison of horizontal and perpendicular printed- parts [8-10]. After dispersion of 4 wt% graphene, it can be noted that elastic modulus of horizontal samples were increased about 32% by addition of graphene while only 8% for perpendicular parts. At the same time, tensile strength of neat ABS is slightly reduced and strain at break was significantly dropped for all building orientation parts. Reduction in strength of H samples was confirmed by poor level of adhesion between graphene and ABS matrix as documented by FESEM micrograph (**Figure 5**b). In addition, the highest reduction is observed for P specimen about 44% and 46% for tensile strength and strain at break, respectively. Fracture occurred between two layers at the gauge length indicating lower bonding strength for graphene nanocomposite. These results suggest that graphene nanofiller play the best reinforcing role when deposited beads parallel to applied load.

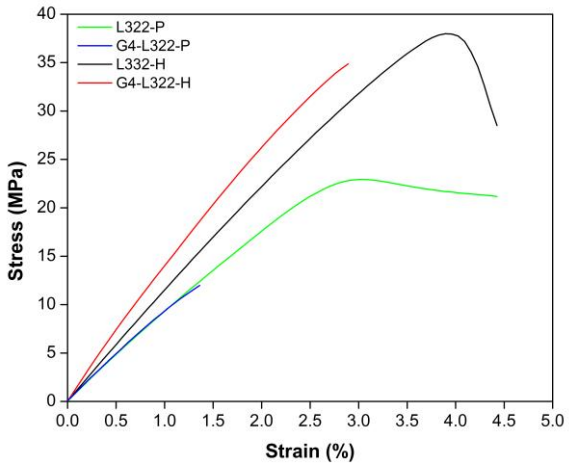

Figure 6. Representative stress-strain curves of 3D-printed specimens with different build orientation.

Table 2. Tensile properties of 3D-printed samples at various build orientation.

Samples	Elastic modulus (GPa)	Yield		Fracture	
		Stress (MPa)	Strain (%)	Stress (MPa)	Strain (%)
L322-P	1.56 ± 0.09	23.8 ± 1.3	2.4 ± 0.1	22.7 ± 2.9	3.3 ± 1.0
G4-L322-P	1.67 ± 0.13	-	-	13.4 ± 1.3	1.8 ± 0.4
L322-H	1.87 ± 0.12	38.8 ± 0.8	3.3 ± 0.1	33.0 ± 4.3	4.2 ± 0.2
G4-L322-H	2.46 ± 0.08	-	-	35.9 ± 1.0	3.0 ± 0.1

Dynamic mechanical analysis was performed in order to evaluate viscoelastic behavior of 3D-printing with various orientations of ABS and graphene composite. Storage modulus (*E*'), loss modulus (E'') and thermal strain of neat ABS and graphene composite along the temperature are plotted in **Figure 7**a and b. In **Table 3** storage modulus at -100, -60, 80, and 140 ºC and intensity of transition are summarized. Horizontally built specimens show higher storage modulus and loss modulus peak than perpendicular specimens, in conformity to tensile Young's modulus. After addition graphene, an increase of *E'* was observed for each building orientation. The glass transition temperature (T_g) of styrene-acrylonitrile (SAN) rigid phase is about 113 ºC, that is slightly increased about 2 °C in the presence of graphene. The positive stiffening effect of graphene nanoplatelets in rubbery state is confirmed by the significant decrease of intensity of transition of storage modulus at T_g. Moreover coefficient of thermal expansion (CTE) of 3D-printed parts is compared in **Table 3**. The neat ABS of H and P specimens have CTE at temperature -40/-10 ºC about 66×10^{-6}/K. Meanwhile at temperature 10/40

Excerpt from ISBN 978-3-00-053387-7

ºC in the range of 65-73×10^{-6}/K. According to literatures, CTE of printed-components were reported as 78-87 ×10^{-6}/K [5, 11]. In **Figure 7**-b, thermal strain curve of H specimen at higher temperate above 130 ºC is observed to be decreased while P specimen showed the positive slope. Different behavior is related to shrinkage of high oriented H-samples above glass transition temperature. After dispersion of graphene, CTE value in the interval temperature of 10/40 ºC is reduced by 28% and 5% for H and P, respectively. The almost negligible effect of graphene on CTE in P specimen could be mainly attributed to the adhesion between layers.

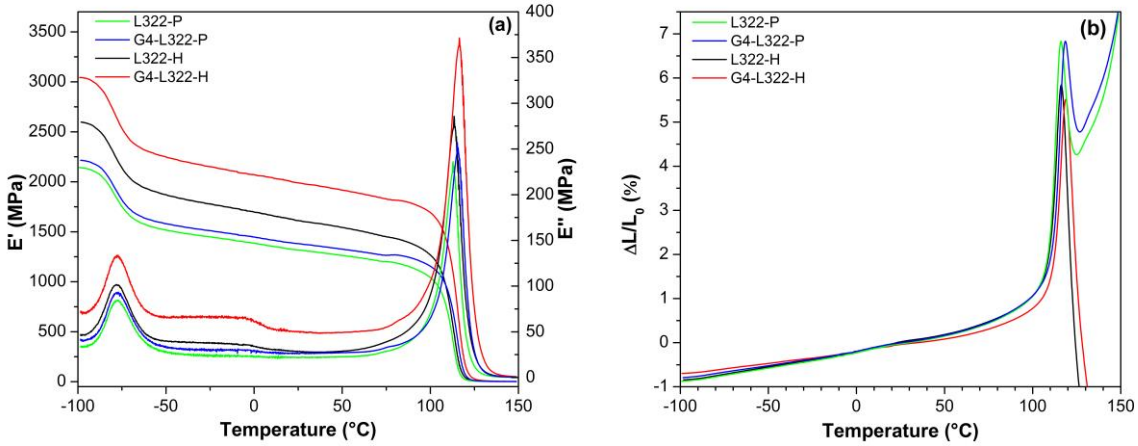

Figure 7. Dynamic mechanical analysis: a) storage modulus (E') and b) thermal strain of neat ABS and nanocomposite samples along different orientation (H and P).

Table 3. Storage modulus, T_g and coefficient thermal expansion for all samples.

Samples	*E'* (MPa)				Intensity of transition		T_g (°C)	CTE (×10^{-6}/K)	
	-100°C	-60°C	80°C	140°C	$\frac{E_{-100°C}}{E_{-60°C}}$	$\frac{E_{80°C}}{E_{140°C}}$		ΔT_1 (-40/-10°C)	ΔT_2 (10/40°C)
L322-P	2144.3	1558.9	1190.7	1.2	1.376	1021.4	113	66.1 ± 0.2	64.9 ± 0.4
G4-L322-P	2217.6	1624.4	1268.2	1.7	1.365	748.3	115	61.2 ± 0.2	61.6 ± 0.3
L322-H	2599.7	1925.7	1433.3	2.0	1.350	701.3	114	64.7 ± 0.2	72.5 ± 0.5
G4-L322-H	3043.2	2303.4	1817.5	3.6	1.321	503.4	116	49.0 ± 0.1	52.6 ± 0.4

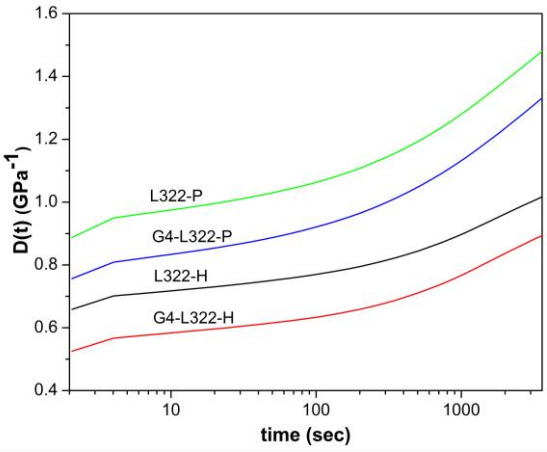

Figure 8. Creep compliance D (t) at 30 ºC of 3D printed specimens for 3600 s.

Figure 8 shows the isothermal creep compliance of ABS and graphene composites at various building orientation. As expected, compliance of neat ABS was reduced by addition of graphene. The role of nanofiller is to restrict the polymeric chain mobility, thus promoting a better creep stability. It is worthy

Excerpt from ISBN 978-3-00-053387-7

to note that horizontal 3D-printed parts exhibited higher reduction of creep compliance than perpendicular specimens. It is suggested that the graphene is effective in promoting the creep stability.

4. Conclusions

Graphene nanoplatelets 4 and 8 wt% were melt compounded into ABS with and without mould lubricant (Sinkral®L322 and Sinkral®F322), and compression moulded specimens were compared under tensile and melt flow index test. The composition at 4 wt% of graphene with lubricated ABS was selected for extrusion of monofilaments suitable for fused deposition modelling. The effect of graphene was investigated under tensile properties, thermal and creep stability along orientation of 3D-printed orientation. During fused deposition modelling, a significant orientation of graphene stacks particles in the flow direction was observed. In any case, tensile modulus of all build orientation was enhanced by the presence of graphene nanoplatelets. Simultaneously, the tensile strength was slightly reduced for horizontal 3D built specimens and had a severe effect along perpendicular specimen. Also addition of graphene promoted the thermal dilation of 3D-printed components. Moreover, creep compliance of printed parts were reduced by this filler. In conclusion, graphene nanoplatelets has been shown to improve properties of ABS, in particular the most relevant reinforcing effect had been observed in horizontally built parts.

Acknowledgments

S. Dul gratefully acknowledges the financial support by Erasmus Mundus Action 2 Programme of European Union AREAS+ project.

References:

[1] T. A. Campbell and O. S. Ivanova, 3D printing of multifunctional nanocomposites, *Nano Today*, 8:119-120, 2013.
[2] A. Duguay, J. Nader, A. Kiziltas, D. Gardner, and H. Dagher, Exfoliated graphite nanoplatelet-filled impact modified polypropylene nanocomposites: influence of particle diameter, filler loading, and coupling agent on the mechanical properties, *Applied Nanoscience*, 4:279-291, 2014.
[3] B. Li and W. H. Zhong, Review on polymer/graphite nanoplatelet nanocomposites, *Journal of Materials Science*, 46:5595-5614, 2011.
[4] T. D. Thanh, L. Kaprálková, J. Hromádková, and I. Kelnar, Effect of graphite nanoplatelets on the structure and properties of PA6-elastomer nanocomposites, *European Polymer Journal*, 50:39-45, 2014.
[5] X. Wei, D. Li, W. Jiang, Z. Gu, X. Wang, Z. Zhang, *et al.*, 3D Printable Graphene Composite, *Scientific Reports*, 5:11181, 2015.
[6] J. Martins, T. Klohn, O. Bianchi, R. Fiorio, and E. Freire, Dynamic mechanical, thermal, and morphological study of ABS/textile fiber composites, *Polymer Bulletin*, 64:497-510, 2010.
[7] L. L. Blyler, The influence of additives on the flow behavior of ABS, *Polymer Engineering & Science*, 14:806-809, 1974.
[8] I. Durgun and R. Ertan, Experimental investigation of FDM process for improvement of mechanical properties and production cost, *Rapid Prototyping Journal*, 20:228-235, 2014.
[9] A. Torrado Perez, D. Roberson, and R. Wicker, Fracture Surface Analysis of 3D-Printed Tensile Specimens of Novel ABS-Based Materials, *Journal of Failure Analysis and Prevention*, 14:343-353, 2014.
[10] S. H. Ahn, M. Montero, D. Odell, S. Roundy, and P. K. Wright, Anisotropic material properties of fused deposition modeling ABS, *Rapid Prototyping Journal*, 8:248-257, 2002.
[11] L. J. Love, V. Kunc, O. Rios, C. E. Duty, A. M. Elliott, B. K. Post, *et al.*, The importance of carbon fiber to polymer additive manufacturing, *Journal of Materials Research*, 29:1893-1898, 2014.

Excerpt from ISBN 978-3-00-053387-7